International Journal of Polymeric Materials and Polymeric Biomaterials, 62: 369–376

ISSN: 0091-4037 print/1563-535X online
DOI: 10.1080/00914037.2012.706839

Taylor & Francis
Taylor & Francis Group

Preparation, Characterization, and Drug-Release Behaviors of a pH-Sensitive Composite Hydrogel Bead Based on Guar Gum, Attapulgite, and Sodium Alginate

HUIXIA YANG[1,2], WENBO WANG[1], JUNPING ZHANG[1], and AIQIN WANG[1]

[1]*R&D Center of Xuyi Attapulgite Applied Technology, Lanzhou Institute of Chemical Physics, Chinese Academy of Sciences, Lanzhou, P. R. China*
[2]*Graduate University of the Chinese Academy of Sciences, Beijing, P. R. China*

Received 6 August 2011, Accepted 24 June 2012

A novel guar gum-***g***-poly (acrylic acid)/attapulgite/sodium alginate (GG-***g***-PAA/APT/SA) composite hydrogel bead with excellent pH sensitivity was prepared via a facile ionic gelation approach and characterized by FTIR and SEM techniques. The effect of APT content on the encapsulation efficiency (EE), swelling ratio, and drug release behaviors of the beads was investigated and the in-vitro release kinetics were also evaluated using diclofenac sodium (DS) as the model drug. The results indicate that the burst release effect of DS drug was eliminated due to the incorporation of APT, and the DS cumulative release was clearly decreased with increasing the APT content.

Keywords: Attapulgite, composite hydrogel bead, drug-release behavior, guar gum, pH-sensitive

1. Introduction

Over the past decades, drug-delivery systems have been the subject of great interest because they can effectively deliver a drug to the target site, maximize the efficacy of drug, minimize the side-effects, and reduce dosing frequency by prolonging the release time [1]. Thus far, numerous technologies and materials have been developed to maximize various benefits of drug-delivery formulations [2,3]. Among them, the ''intelligent'' or ''smart'' hydrogels have received considerable attention in drug-delivery systems because they can regulate drug release through the volume phase change of gel induced by the environmental stimuli, such as pH, temperature, ionic strength, and electric field [4,5]. A pH-sensitive hydrogel can rapidly response to the external pH stimuli, and was developed as the most effective carrier of gastrointestinal drugs [6]. Hence, the pH-sensitive hydrogels were produced from various sources as promising, intelligent drug-delivery systems [7–9], and the polysaccharide-based systems show a unique prospect by virtue of their advantages such as non-toxicity, inexpensive, biodegradability, and biocompatibility [10,11].

Guar gum (GG) is a naturally occurring, non-ionic, water-soluble polysaccharide derived from the seeds of *Cyamopsis tetragonolobus*, and it consists of linear chains of (1→4)-β-D-manopyranosyl units with α-D-galactopyranosyl units attached by (1→6) linkages. There are $1.5 \sim 2$ mannose residues for every galactose residue. GG and its derivatives have been extensively applied in various areas (e.g., cosmetics, food, drug-delivery and health care products, etc.), due to their natural abundance, low price, and immense potential [12]. In pharmaceutical formulations, GG has been developed as an effective drug vehicle for use as matrices [2,13,14], tablets [15,16], microspheres [17,18], etc., for the controlled release of various drugs. Also, GG may be used in colon-specific drug delivery owing to its drug-release retarding property and susceptibility to microbial degradation in the large intestine [19,20]. The existence of reactive –OH groups of GG makes it easily modified to introduce functional groups, and thus the capabilities for controlling the release of drugs can be improved. For example, the GG derivatives containing carboxymethyl groups [21], polyacrylamide groups [22], and phosphate groups [23], etc., have all showed excellent drug-delivery properties. In addition, GG and its derivatives had been crosslinked with Ca^{2+} and Ba^{2+}[21], glutaraldehyde [24,25], and trisodium trimetaphosphate (STMP) [23], and grafted with gumpoly(ε-caprolactone) [26] to improve its property profiles for a wide range of biomedical applications [27].

Biopolymer/clay composites as controlled drug-delivery vehicles have drawn much attention owing to their unique structure and properties [28]. The synergistic effect of biopolymer and clay as well as the strong interfacial interactions between them (e.g., electrostatic and hydrogen bonding interaction) could improve the mechanical properties, swelling

Address correspondence to: Aiqin Wang, Lanzhou Institute of Chemical Physics, Chinese Academy of Sciences, Lanzhou 730000, P. R. China. E-mail: aqwang@licp.cas.cn

behavior, drug-loading efficiency, and controlled release behavior of the pristine biopolymer matrices [29]. The chitosan/montmorillonite nanohydrogel composites were demonstrated to exhibit excellent anti-fatigue behavior and better pulsatile release compared with neat chitosan [30]. Furthermore, our groups have reported that the introduction of vermiculite [31] and attapulgite [32] into a CTS-*g*-PAA polymeric network can eliminate the burst-release effect of the drug. Attapulgite (APT) is a kind of hydrated, octahedral, layered magnesium aluminum silicate mineral with exchangeable cations in its framework channels and reactive −OH groups on its surface. It is a type of natural fibrous silicate clay, consisting of two double chains of the pyroxene-type $(SiO_3)^{2-}$ like amphibole $(Si_4O_{11})^{6-}$ running parallel to the fiber axis. It can participate in a polymerization reaction by its active silanol groups to derive new hybrid materials [33]. It is expected that a composite of GG with APT could improve the type and number of functional groups, the network structure, and drug-delivery properties.

Based on the above background, the new drug-delivery system combined the pH-sensitive guar gum-*g*-poly (acrylic acid)/attapulgite (GG-*g*-PAA/APT) composite hydrogel with the pH-sensitive SA was designed and developed for the delivery of DS. The influences of APT content on the swelling property, encapsulation efficiency, and in-vitro drug release pattern of the developed beads were investigated. In addition, the release dynamics were evaluated systematically and the release mechanism was revealed.

2. Materials and Methods

2.1 Materials

GG (food grade, number average molecular weight 220,000) was obtained from Wuhan Tianyuan Biology Co., China. Acrylic acid (AA, chemically pure, distilled under reduced pressure before use) was purchased from Shanghai Wulian Chemical Factory (Shanghai, China). Ammonium persulfate (APS, analytically pure, recrystallized before use) was purchased from Xi'an Chemical Reagent Factory (Xi'an, China) and *N, N'*-methylenebisacrylamide (MBA, chemically pure) was purchased from Shanghai Chemical Reagent Corporation (Shanghai, China). APT clay micropowder (Linze Colloidal Co., Gansu, China) was milled and passed through a 320-mesh screen prior to use. Sodium alginate (SA) was purchased from Shanghai Chemical Co. Ltd. (Shanghai, China). Diclofenac sodium (DS) was purchased from Jiuzhou Pharmaceutical Factory (He'nan, China). All the other reagents used were of analytical grade and all solutions were prepared with distilled water.

2.2 Preparation of GG-g-PAA/APT and GG-g-PAA Hydrogels

GG-*g*-PAA/APT composite hydrogels were prepared according to our previous report [34]. 1.2 g of GG was dispersed in 34 mL of NaOH solution (pH 12.5, 0.067 mol/L; calculated as a part of the neutralization degree) in a 250 mL four-necked flask equipped with a mechanical stirrer, a reflux condenser, a thermometer, and a nitrogen line. The dispersion was heated to 60°C in an oil bath and stirred for 1 h to form a colloidal slurry, then an aqueous solution (4 mL) containing 0.1 g initiator APS was added and the mixture was stirred for 10 min to generate the radicals. After the reactants were cooled to 40°C, 17 mL of the mixed solution containing 7.2 g of AA neutralized with 8.5 mL of NaOH solution (8.0 mol/L), 21.6 mg MBA, and a calculated amount of APT powder was added. Then, the oil bath was slowly heated to 70°C and kept for 3 hr. A nitrogen atmosphere was maintained throughout the reaction period. The obtained gels were dried in an oven at 70°C to a constant weight and ground to a desired size (>200 mesh). The preparation procedure of GG-*g*-PAA is similar to that described above except without the addition of APT.

2.3 Preparation of GG-g-PAA/APT/SA Composite Hydrogel Beads

The GG-*g*-PAA/APT/SA composite hydrogel beads were prepared by the ionic crosslinking gelation technique. A predetermined amount of DS was added into the dispersion of GG-*g*-PAA/APT and stirred at 30°C for 2 h to achieve a full penetration of DS molecules into the GG-*g*-PAA/APT hydrogel. Then, an appropriate amount of SA was added and further stirred at 1000 rpm for 4 h to obtain a homogeneous mixture before the crosslinking procedure. After removing the bubbles, the mixture was dropped into a gently stirred $CaCl_2$ solution at the rate of 1.50 mL/min using a 0.45 mm syringe needle. The GG-*g*-PAA/APT/SA composite hydrogel beads were formed instantaneously and crosslinked with Ca^{2+} in solution for further 2 h. The obtained hydrogel beads were rinsed with distilled water for three times to remove unreacted $CaCl_2$ on the surface, dried at room temperature for 24 h, and subsequently dried at 70°C in an oven to a constant weight.

2.4 Measurement of Swelling Ratio and pH Sensitivity

A total of 0.20 g of the sample was soaked in the baskets of intelligent dissolution apparatus (ZRS-8 G, Tianjing University Wireless Factory, China) containing 250 mL pH 6.8 phosphate buffer solution (PBS) at 37 ± 1°C and stirred at 50 rpm. After a predetermined time interval, the swollen samples were separated out using a 100-mesh screen under gravity for 30 min without blotting the samples. Swelling ratio of the samples at given time is defined as grams of water absorbed by per gram of sample and can be calculated using the following equation:

$$\text{Swelling ratio} = \frac{W_s - W_d}{W_d} \quad (1)$$

Where W_s and W_d is the weight of the swollen beads and dry beads at time t, respectively.

The buffer solutions of various pHs, which were used to study the pH sensitivity of the composite hydrogel beads, were made by properly combining NaH_2PO_4, Na_2HPO_4, NaCl, and NaOH solutions. The pH value was precisely checked by a pH meter (DELTA-320) and ionic strengths

were adjusted as 0.2 mol/L using NaCl. Then, swelling ratio in solutions of various pHs was tested according to the procedure described above.

2.5 Determination of Encapsulation Efficiency and Drug Loading

A total of 50 mg of the composite hydrogel beads was incubated in 25 mL of pH 6.8 PBS in a 50 mL beaker for complete swelling. The swollen beads were crushed in a mortar with a pestle and transferred into a conical flask, approximately 10 mL of the fresh PBS was added to the conical flask, and the resultant mixture was sonicated for 20 min. After centrifugation (5000 rpm for 20 min), 2 mL of the supernatant was transferred into a 25 mL flask. The clear solution was then assayed using a UV-vis spectrophotometer (Specord 200, Analytik Jena AG) at the fixed wavelength (λ_{max}) of 276 nm. The percentage drug loading (DL, %) and percentage encapsulation efficiency (EE, %) were calculated using the following equations, respectively:

$$\text{Drug Loading (\%)} = \frac{\text{Weight of drug in hydrogel beads}}{\text{Weight of hydrogel beads}} \times 100 \quad (2)$$

$$\text{Encapsulation efficiency (\%)} = \frac{\text{Weight of drug in hydrogel beads}}{\text{Theoretical drug loading}} \times 100 \quad (3)$$

2.6 in Vitro Drug Release

In-vitro release behaviors of DS were performed in an intelligent dissolution apparatus equipped with six paddles. 0.2 g of the dried DS-loaded composite hydrogel beads were immersed in 500 mL dissolution media (pHs 1.2, 5.8, or 6.8) and obtained the sink condition. The mixture was kept at 37 ± 1°C under 50 rpm paddle speed. At a set time interval, 5 mL of the solution was withdrawn and replaced with an equal amount of fresh dissolution media to maintain a constant volume. The collected solution (5 mL) was filtrated through a 0.45 μm membrane, and we determined the concentration of DS by a UV-*vis* spectrophotometer at 276 nm. The amount of DS released at each time point was calculated according to the standard curve of DS in PBS (pHs 1.2, 5.8, or 6.8) and was expressed as μg/mL. The accumulative release percent (average of three measurements) was used to evaluate the release rate.

The sequential release properties of DS were tested as follows: The dried test sample was immersed in dissolution media of pH 1.2 for initial 2 h (the average gastric emptying time is about 2 h [35]) and subsequently replaced with pH 6.8 PBS at 37 ± 1°C. At predetermined time points, the percentage of cumulative amount of released DS was determined as previously described.

2.7 Characterization

FTIR spectra of the hydrogel beads were taken as KBr pellets using a Thermo Nicolet NEXUS TM spectrophotometer. Micrographs of the hydrogel beads were taken using scanning electron microscopy (JSM-5600LV, JEOL, Ltd.) after coating the sample with gold film.

2.8 Statistical Analysis

All values were expressed as their average ±S.D. One-way analysis of variance test (ANOVA) was also performed to check whether there was significant difference among the different formulations and a value of $P < 0.05$ was statistically significant.

3. Results and Discussion

3.1 Encapsulation Efficiency (EE) and Drug Loading (DL) of the Composite Hydrogel Beads

The effect of APT content on the EE and DL of the composite hydrogel beads with different contents of APT was investigated under the optimized conditions (Table 1). As can be seen, the EE and DL of the beads decreased with increasing content of APT. This may be attributed to the following facts. Firstly, the introduced APT can generate a rough and lacunaris surface with large wrinkles, which facilitates the escape of DS during the sol-gel transition of SA. Secondly, APT nano-rods could react with AA and GG as crosslinking points, which increased the crosslinking density of the composite hydrogel [34] and then decreased the EE and DL. These findings are similar to the results reported previously by Wang et al. [31].

3.2 FTIR Spectra Analysis

In this study, the GG-*g*-PAA/APT nanocomposite was utilized to construct drug carriers for extending its application fields. However, the burst effect of the drug loaded in the nanocomposites was obviously observed according to the results of preliminary experiments [36]. In order to solve this problem, SA was introduced to the GG-*g*-PAA/APT hydrogel, and the contact between SA and Ca^{2+} in solution immediately induces ionic crosslinking of alginate, and then forms the hydrogel beads.

Table 1. Preparation conditions of GG-g-PAA/APT/SA composite hydrogel beads and their influence on Encapsulation Efficiency (EE) and drug loading (DL)

Sample	DS (g)	GG-*g*-AA/APT (g)	SA (g)	$CaCl_2$ (%)	EE	DL
GG-*g*-AA/SA	0.5	0.5	1.0	5	0.712	0.165
GG-*g*-AA/5%APT /SA	0.5	0.5	1.0	5	0.682	0.158
GG-*g*-AA/10%APT/SA	0.5	0.5	1.0	5	0.678	0.157
GG-*g*-AA/30%APT/SA	0.5	0.5	1.0	5	0.641	0.155

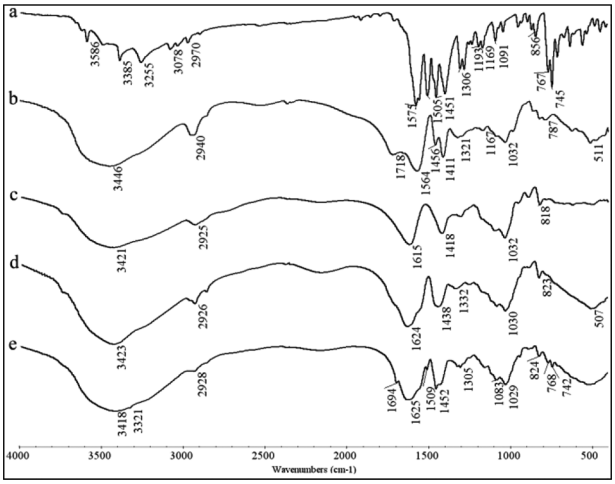

Fig. 1. FTIR spectra of (a) DS; (b) GG-*g*-PAA/30% APT; (c) SA; (d) GG-*g*-PAA/30%APT/SA; and (e) DS-loaded GG-*g*-PAA/30% APT/SA.

The FTIR spectra of (a) DS, (b) GG-*g*-PAA/30% APT, (c) SA, (d) GG-*g*-PAA/30%APT/SA, and (e) DS-loaded GG-*g*-PAA/30%APT/SA are shown in Figure 1. In the FTIR spectrum of GG-*g*-PAA/30% APT (Figure 1b), the characteristic absorption bands at 1718, 1564, and $1456 \sim 1411\,cm^{-1}$ are ascribed to stretching vibration of C = O, asymmetric and symmetric stretching vibrations of the $–COO^-$ groups on the polymeric backbone. After combination of SA into the GG-*g*-PAA/30% APT network and crosslinking by Ca^{2+}, the characteristic absorption band of SA at 1615 and $1418\,cm^{-1}$ (Figure 1c) was enhanced and shifted to 1624 and $1438\,cm^{-1}$, respectively (Figure 1d). This is attributed to the ionic bonding between $–COO^-$ groups of DS molecules and Ca^{2+} ions in GG-*g*-PAA/APT/SA bead and electrostatic interaction of DS and SA [31]. Furthermore, the observed new bands at $1509 \sim 1452$ and $768 \sim 742\,cm^{-1}$ in the spectrum DS-loaded GG-*g*-PAA/30% APT/SA are attributed to the stretching and bending vibration of benzene ring of DS compared with the spectra of non-DS-loaded GG-*g*-PAA/30% APT/SA and DS, respectively. Moreover, the strong absorption bands at $1505\,cm^{-1}$ and $1451\,cm^{-1}$ of the DS molecule in Figure 1(a) appear in the spectrum of the DS-loaded GG-*g*-PAA/APT/SA bead with slight shift, which indicates that the DS molecules are successfully entrapped into GG-*g*-PAA/30% APT/SA composite hydrogels.

3.3 Morphological Analysis

SEM is the most widely employed technique to investigate the shape, size, and porosity of the hydrogels [37]. To investigate the influence of APT on resultant hydrogel beads, the surface morphology of GG-*g*-PAA/SA and GG-*g*-PAA/APT/SA bead were also investigated in this section by SEM, as shown in Figure 2. Most of the DS-loaded GG-*g*-PAA/APT/SA beads are spherical in shape with a smooth surface, and the sizes are around 4.0–5.0 mm in a swollen state (Figure 2(a)), whereas the dried beads had a rough

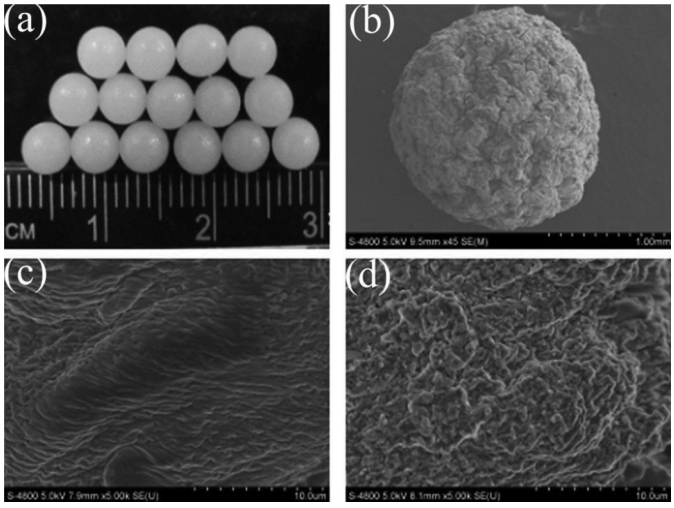

Fig. 2. Digital photo of (a) GG-*g*-PAA/APT/SA hydrogel beads at swollen state; SEM micrographs of (b) GG-*g*-PAA/APT/SA hydrogel bead at dry state; (c) GG-*g*-PAA/SA hydrogel bead (×5000); and (d) GG-*g*-PAA/APT/SA hydrogel bead (×5000).

and lacunaris surface with large wrinkles (Figure 2(b)). In addition, the GG-*g*-PAA/SA bead shows a compact surface (Figure 2(c)), whereas a loose surface (Figure 2(d)) is observed for the GG-*g*-PAA/10%APT/SA bead. The surface morphology changing by introducing APT may have some influence on swelling abilities and the release behaviors of DS from the bead [32].

3.4 Effect of pH on Swelling Ratio

In the present study, the effect of pH on swelling ratio of the resultant beads was evaluated by varying pH of the release medium. The maximal swelling ratio of the GG-*g*-PAA/APT/SA bead is shown in Figure 3. It is

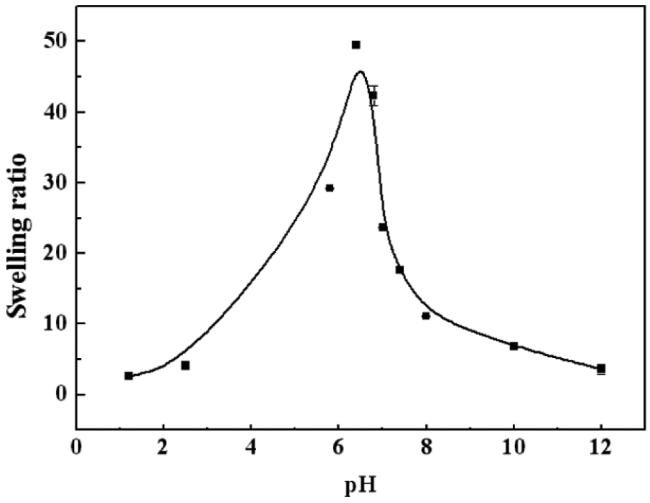

Fig. 3. Variation of swelling ratio for GG-*g*-PAA/APT/SA composite hydrogel beads at various pHs at 37°C. APT content is 10 wt%. Weight ratio of GG-*g*-PAA/APT to SA is 1:2. $CaCl_2$ concentration is 7% (w/v).

observed that the swelling ratio of the bead is very small when the pH is lower than 5.0, and then increases sharply to 48 ± 0.39 with increasing pH to 6.8, but then decreases to 5 ± 0.21 with further increasing pH to 12.0. Because of containing anionic carboxyl and hydroxyl groups in the matrix, the swelling could be controlled by the pH. When $pH \leq 2.0$, $-COO^-$ groups convert to –COOH groups and form hydrogen bonding with –OH groups, which is responsible for the small swelling ratio. When the pH of the solution increases gradually to pH 6.8, most of the -COOH groups change into $–COO^-$ groups and the hydrogen bonding among –COOH and –OH groups dissociates among the –COOH and –OH groups. As a consequence, the electrostatic repulsion within the test beads makes the hydrogel dramatically swell. However, when $pH > 6.8$, the swelling ratio decreases, which may be ascribed to the cracking of the bead due to the reaction of PO_4^{3-} and Ca^{2+} in the basic region [31]. The characteristic for variation of swelling ratio with pH of external buffer solution illustrates the good pH responsive behavior of the GG-*g*-PAA/APT/SA bead.

3.5 Effect of APT Content on Swelling Ratio

Swelling ratio is a very important property for the hydrogels because of its great influence on their practical application, such as a drug-delivery vehicle. Hence, the effect of APT content on swelling ratio of the GG-*g*-PAA/APT/SA bead in pH 6.8 PBS was investigated and is shown in Figure 4. It is obvious that the swelling ratio of the GG-*g*-PAA/APT bead decreases with increasing APT content from 0 wt.% to 30 wt.%. The behavior may be attributed to the reaction among GG, AA, and APT. The addition of APT results in the generation of more crosslinking points that increase the crosslinking density of the bead, and then the elasticity of the polymer chains decreases. As a result, the swelling ratio decreases. Moreover, the content of hydrophilic groups is lower at higher APT content, and then the osmotic pressure difference decreases, which results in the shrinkage of the GG-*g*-PAA/APT/SA bead and the swelling ratio also decreases. A similar phenomenon was also observed by Wang et al. [34]. The changes of swelling behavior of the GG-*g*-PAA/APT/SA bead by introducing APT may be also beneficial to the drug-controlled release.

3.6 Effect of pH on Release of DS

It is known that the natural pH environment of the gastrointestinal tract varies from acidic (pH is about $1.2 \sim 2.0$) in the stomach to slightly alkaline (pH about 7.4) in the intestine. Thus pH is a key factor which is a highly significant parameter controlling drug-release behavior in pH-sensitive hydrogels. The effect of pH on the release rate of DS from the bead is shown in Figure 5. When pH of the medium is 1.2, the cumulative release ratio of DS from the bead is below 2% at the end of the experiment (24 h). At pH 5.8, the drug cumulative release ratio is 22.96%, 50.07%, and 57.79% after 5 h, 12 h, and 24 h, respectively, whereas the drug cumulative release ratio is 60.76%, 79.69%, and 85.12% at pH 6.8 after 5 h, 12 h, and 24 h, respectively. Obviously, the release of DS of the same APT content at pH 1.2 and 5.8 is slower than that at pH 6.8 and the variation is attributed to the following facts. With changing pH of the medium, their swelling behavior varied as described in the previous swelling experiment. The release of the water-soluble drug from the swellable matrix occurs only after the penetration of water into the polymeric matrix, which allows swelling of the polymer and drug dissolution, following diffusion along the pathway to the solution [18]. As a result, it is very difficult for the DS to migrate out of the bead at pH 1.2 since the swelling ratio is very small. However, the swelling of the bead increases at pH 5.8 or 6.8. Consequently, there is enough space among the polymer

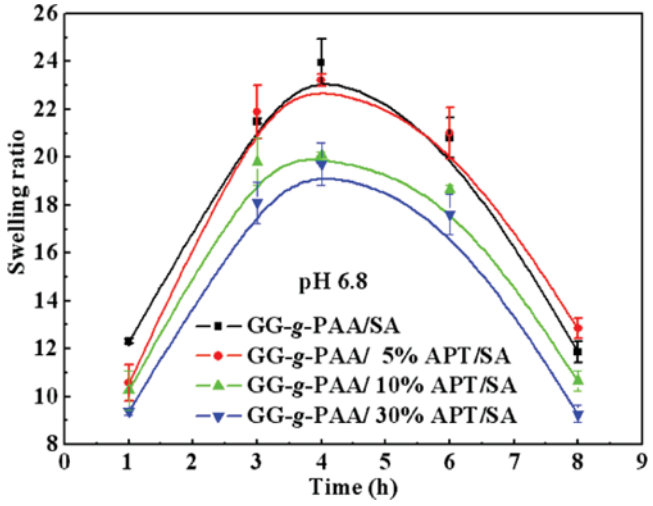

Fig. 4. The influence of APT content on the swelling ratio for GG-*g*-PAA/APT/SA composite hydrogel beads at 37°C. Weight ratio of GG-*g*-PAA/APT to SA is 1:2. $CaCl_2$ concentration is 7% (w/v). (Figure is provided in color online.)

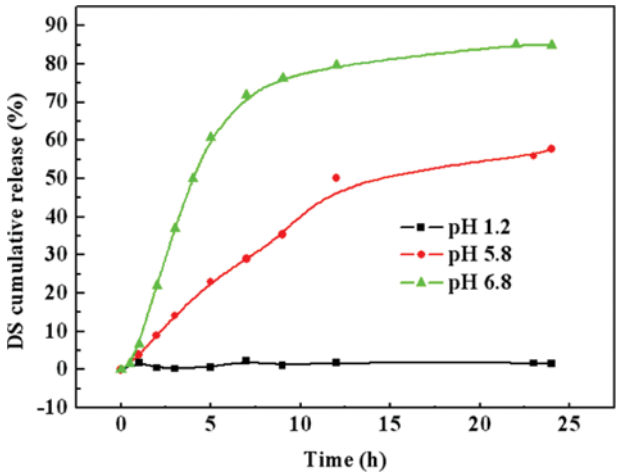

Fig. 5. The cumulative release curves of DS from GG-*g*-PAA/APT/SA composite hydrogel beads at various pHs at 37°C after 24 h. APT content is 10%. Weight ratio of GG-*g*-PAA/APT to SA is 1:2. $CaCl_2$ concentration is 7% (w/v). (Figure is provided in color online.)

chains of the bead, which facilitates migration of DS out of the beads, and then the evident release of DS was observed. In addition, the GG-*g*-PAA/APT/SA bead hardly cracks after DS releasing for 24 h at pH 1.2, while the bead ruptures after releasing for 5 h at pH 6.8. A similar phenomenon also was observed by Shu [38].

3.7 *Effect of APT Content on Release of DS*

Figure 6 shows the time-dependent cumulative release of the drug from the hydrogel beads with different APT content in a pH 6.8 buffer solution. As can be seen from Figure 6, with increase in swelling time, the DS cumulative release ratio from GG-*g*-PAA/SA bead is increased from 30.27% (2 h) to 76.23% (5 h), and up to 94.93% throughout the observation period (24 h), which is due to rapid hydration and swelling [18]. However, as APT content increased to 30%, the DS cumulative release ratio increased from 16.85% (at 2 h) to 45.53% (at 5 h), and up to 73.14% after 24 h, which is slower than the GG-*g*-PAA/SA bead. This may be attributed to the role that APT plays in the GG-*g*-PAA/APT/SA bead [39]. The DS adsorbed on APT need to be firstly desorbed, and then migrate out of the bead through a longer path. In other words, the existence of APT improved the release behavior as observed in Figure 6.

To further examine the sequential release of DS from the GG-*g*-PAA/APT/SA bead in stimulated gastric fluids and intestinal fluids, the beads were suspended in stimulated gastric fluids (pH 2.1) for an initial 2 h, and then moved to stimulated intestinal fluids (pH 6.8). The results are shown in Figure 7. In stimulated gastric fluids (pH 2.1), the drug cumulative release ratio of DS from the GG-*g*-PAA/SA is not more than 1.74% within 2 h. However, when transferred to stimulated intestinal fluids (pH 6.8), it is increased quickly to 75.53% after 1 h, and up to 77.69% after 8 h. Furthermore, the cumulative release was reduced obviously with increasing

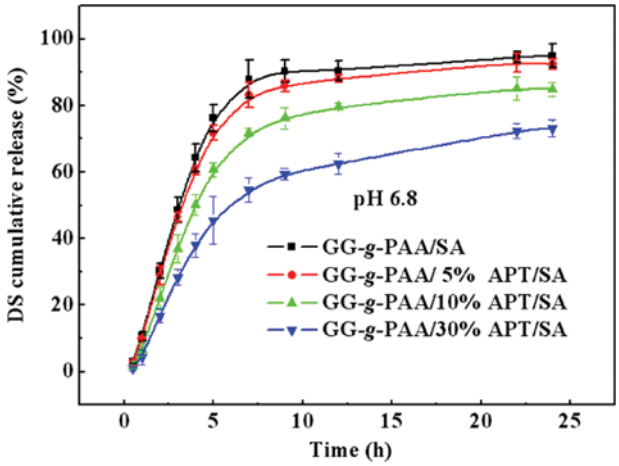

Fig. 6. In-vitro cumulative release curves of DS from GG-*g*-PAA/APT/SA composite hydrogel beads with different APT content at 37°C after 24 h. Weight ratio of GG-*g*-PAA/APT to SA is 1:2.$CaCl_2$ concentration is 7% (w/v). (Figure is provided in color online.)

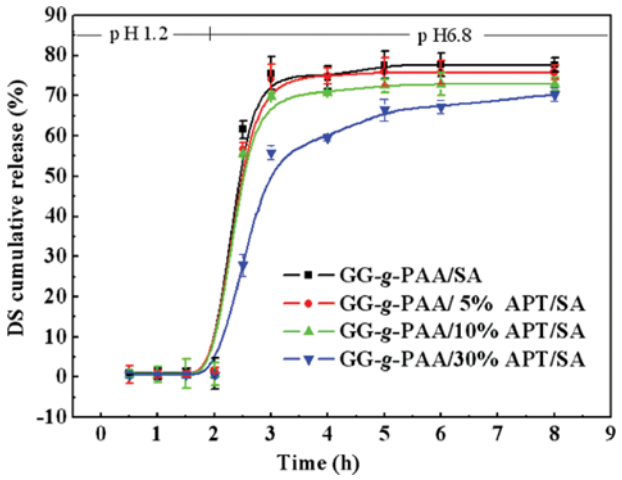

Fig. 7. The sequential cumulative release curves of DS from GG-*g*-PAA/APT/SA composite hydrogel beads in SGF (pH 1.2) for initial 2 h and then moved to SIF (pH 6.8) at 37°C. (Figure is provided in color online.)

APT content. The very low release percentage at pH 2.1 is due to its shrinking behavior, whereas the quick release of DS at pH 6.8 is because the swelling of the bead increases considerably. Therefore, the GG-*g*-PAA/APT/SA beads are good candidates as a drug-delivery system in the intestinal tract, and incorporating APT into the resultant beads could improve the burst release effect.

3.8 *Empirical Analysis of in Vitro Release Data*

In order to describe the kinetics of release parameters of drug in the formulations, various equations were fitted and correlation coefficients along with other statistical parameters were estimated [2]. According to zero-order release, which describes the systems where the release rate is independent of the concentration of the dissolved species [40], the equation is shown as follows:

$$Q = Q_0 - K_0 t \tag{4}$$

where Q is the amount of drug at time t, Q_0 is the amount of drug at $t = 0$, and K_0 is the zero-order release constant. The first-order equation describes the release from systems where dissolution rate is dependent on the concentration of the dissolving species, which is shown as follows:

$$\ln Q = \ln Q_0 - K_1 t \tag{5}$$

where K_1 is the first-order release constant. The Higuchi square-root equation describes the release from systems where the solid drug is dispersed in an insoluble matrix and the rate of drug release is related to the rate of drug diffusion, which is given as follows [41]:

$$\ln M_t = \ln K_H + 0.5 \ln t \tag{6}$$

where M_t is the amount of drug released at time t and K_H is the Higuchi rate constant.

From the analysis of release kinetics using empirical equations as reported in Table 2, it was found that the fit

Table 2. Kinetic analyses of the GG-*g*-PAA/APT/SA composite hydrogel beads

	Release models and release parameters						
	Zero order		First order		Higuchi		
Samples	K_0	R	K_1	R	K_H	R	t_{50}
GG-*g*-AA/SA	0.0849	0.9074	0.2329	0.9572	0.3601	0.9587	3.47
GG-*g*-AA/5%APT/SA	0.0818	0.9154	0.2022	0.9684	0.3468	0.9650	3.75
GG-*g*-AA/10%APT/SA	0.0747	0.9346	0.1499	0.9732	0.3181	0.9759	4.74
GG-*g*-AA/30%APT/SA	0.0585	0.9424	0.0912	0.9659	0.2492	0.9810	6.99

was better with the Higuchi equation than with the other equations, and the increase of the t_{50} values with the increase of APT content from 3.47 h to 6.99 h indicates that APT could slow down the drug release of the bead.

In order to prove the relationship of the swelling ratio and the cumulative release ratio, the following empirical equations were used to estimate the drug-release mechanism of the test beads with various APT contents. According to the Peppas Power law [42]:

$$\ln(M_t/M_\infty) = \ln k + n \ln t \quad (7)$$

where M_t/M_∞ represents the fractional drug release at time t, k is a kinetic constant characterizing the drug-polymer interaction, and n is an empirical parameter characterizing the transport mechanism. For spheres, when $n < 0.43$, this represents a Fickian diffusion mechanism. When $n > 0.89$, a Case II transport mechanism is operative in which drug release from the sphere is zero-order, whereas n is between 0.43 and 0.89, the mechanism is anomalous transport. The relationship between $\ln(M_t/M_\infty)$ and $\ln t$ is given in Figure 8. The fitting result of the calculated values of k and n parameters of the cumulative release data of DS loaded in the composite hydrogel beads with different APT content is listed in Table 3. The release constant k is found to decrease when APT was introduced. The n values also gradually increased from 0.8555 to 0.9588, and the release mechanism of the drug was varied from anomalous transport to Case-II transport with increasing the content of APT from 0 wt.% to 30 wt.%.

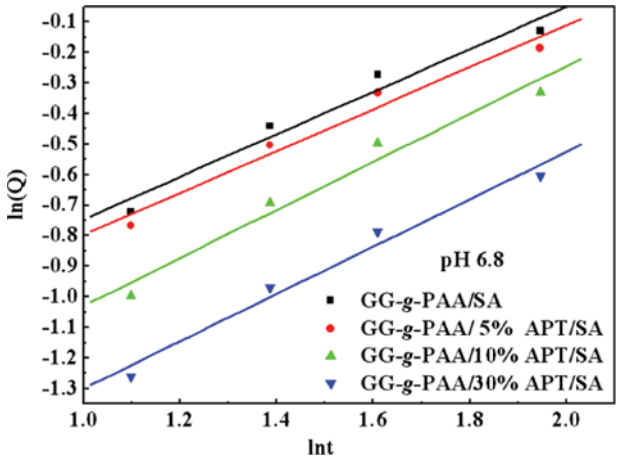

Fig. 8. The plot of $\ln(Q)$ vs. $\ln t$ for the fitting using Ritger-Peppas model. (Figure is provided in color online.)

Table 3. Release mechanism of DS-loaded GG-*g*-PAA/APT/SA hydrogel beads with different APT content

Samples	n[a]	k[b]	r[c]	Drug transport mechanism
GG-*g*-AA/SA	0.8555	0.1799	0.9815	Anomalous transport
GG-*g*-AA/5%APT/SA	0.8638	0.1723	0.9822	Anomalous transport
GG-*g*-AA/10%APT/SA	0.9477	0.1228	0.9940	Case-II transport
GG-*g*-AA/30%APT/SA	0.9588	0.9475	0.9851	Case-II transport

[a]diffusional exponents;
[b]kinetic constants;
[c]correlation coefficients.

Conclusions

In this study, novel pH-sensitive GG-*g*-PAA/APT/SA composite hydrogel beads were successfully prepared by a facile ionic gelation method, and the optimum formulation was obtained by orthogonal design. FTIR results indicate that DS dispersed in the GG-*g*-PAA/APT/SA beads by physical blend. SEM observation indicates that the composite hydrogel beads have a rough and lacunaris surface when the content of APT is above 10 wt.%. From the results obtained in this work, it can be concluded that a significant variation exists in the in-vitro release pattern of DS from the tested formulations. In addition, the release rate of DS from the beads can be simply regulated by changing APT content. The higher the APT concentration is, the lower the swelling ratio. Consequently, the DS cumulative release rate was slowed down. Clearly, incorporating APT into the hydrogel beads could control the release rate and the burst release effect of the drug can be effectively eliminated.

Acknowledgements

The authors are thankful for the joint support of the National Natural Science Foundation of China (No. 51003112) and the Science and Technology Support Project of Jiangsu Provincial Science & Tech. Department (No. BY2010012).

References

1. Ranade, V. V.; Hollinger, M. A. *Drug Delivery Systems*; CRC Press: Boca Raton, FL, 1995.
2. Sullad, A. G.; Manjeshwar, L. S.; Aminabhavi, T. M. *Ind. Eng. Chem. Res.* **2010**, *49*, 7323.
3. Namazi, H.; Jafarirad, S. *Int. J. Polym. Mater.* **2011**, *60*, 603.
4. Liu, L.; Sheardown, H. *Biomaterials* **2005**, *26*, 233.
5. Zhang, X. Z.; Wu, D. Q.; Chu, C. C. *Biomaterials* **2004**, *25*, 3793.
6. Gupta, P.; Vermani, K.; Garg, S. *Drug Discov. Today* **2002**, *7*, 569.
7. Griset, A. P.; Walpole, J.; Liu, R.; Gaffey, A.; Colson, Y. L.; Grinstaff, M. W. *J. Am. Chem. Soc.* **2009**, *131*, 2469.
8. O'Halloran, T. V.; Lee, S. M.; Chen, H.; Dettmer, C. M.; and Nguyen, S. T. *J. Am. Chem. Soc.* **2007**, *129*, 15096.
9. Yang, S. P.; Fu, S. Y.; Zhou, Y. M.; Xie, C. L.; Li, X. Y. *Int. J. Polym. Mater.* **2010**, *60*, 52.
10. George, M.; Abraham, T. E. *Int. J. Pharm.* **2007**, *335*, 123.
11. Maji, T. K.; Devi, N. *Int. J. Polym. Mater.* **2010**, *59*, 828.
12. Khan, S. A.; Mahammad, S.; Prud'homme, R. K.; Roberts, G. W. *Biomacromolecules* **2006**, *7*, 2583.
13. Sen, G.; Mishra, S.; Jha, U.; Pal, S. *Int. J. Bio. Macromol.* **2010**, *47*, 164.
14. Baloglu, E.; Senyigit, T. *AAPS PharmSciTech* **2010**, *11*, 563.
15. Jain, N. K.; Kulkarni, K.; Talwar, N. *Pharmazie* **1992**, *47*, 277.
16. Prasad, Y. V. R.; Krishnaiah, Y. S. R.; Satyanarayana, S. *J. Control. Release* **1998**, *51*, 281.
17. Chaurasia, M.; Chourasia, M. K.; Jain, N. K.; Jain, A.; Soni, V.; Gupta, Y.; Jain, S. K. *AAPS PharmSciTech* **2006**, *7*, E143.
18. Kumar, S. R.; Piyush, T.; Suman, R.; Akanksha, T. *Chem. & Pharm. Bull.* **2011**, *59*, 185.
19. Krishnaiah, Y. S. R.; Satyanarayana, S.; Prasad, Y. V. R.; Rao, S. N. *J. Control. Release* **1998**, *55*, 245.
20. Krishnaiah, Y. S. R.; Muzib, Y. I.; Rao, G. S.; Bhaskar, P.; and Satyanarayana, V. *Drug Delivery* **2003**, *10*, 111.
21. Thimma, R. T.; Tammishetti, S. *J. Appl. Polym. Sci.* **2001**, *82*, 3084.
22. Soppimath, K. S.; Kulkarni, A. R.; Aminabhavi, T. M. *J. Control. Release* **2001**, *75*, 331.
23. Gliko-Kabir, I.; Yagen, B.; Baluom, M.; Rubinstein, A. *J. Control. Release* **2000**, *63*, 129.
24. Sandolo, C.; Matricardi, P.; Alhaique, F.; Coviello, T. *Food Hydrocolloids* **2009**, *23*, 210.
25. Gliko-Kabir, I.; Yagen, B.; Penhasi, A.; Rubinstein, A. *Pharm. Res.* **1998**, *15*, 1019.
26. Tiwari, A.; Prabaharan, M. *J. Biomater. Sci. Polym. Ed.* **2010**, *21*, 937.
27. Rana, V.; Rai, P.; Tiwary, A. K.; Singh, R. S.; Kennedy, J. F.; Knill, C. J. *Carbohyd. Polym.* **2011**, *83*, 1031.
28. Viseras, C.; Aguzzi, C.; Cerezo, P.; Bedmar, M. C. *Mater. Sci. Technol.* **2008**, *24*, 1020.
29. Zhang, J. P.; Wang, Q.; Xie, X. L.; Li, X.; Wang, A. Q. *J. Biomed. Mater. Res. B Appl. Biomater.* **2010**, *92B*, 205.
30. Liu, K. H.; Liu, T. Y.; Chen, S. Y.; Liu, D. M. *Acta Biomater.* **2008**, *4*, 1038.
31. Wang, Q.; Xie, X. L.; Zhang, X. W.; Zhang, J. P.; Wang, A. Q. *Int. J. Bio. Macromol.* **2010**, *46*, 356.
32. Wang, Q.; Zhang, J. P.; Wang, A. Q. *Carbohyd. Polym.* **2009**, *78*, 731.
33. Wang, W. B.; & Wang, A. Q. *Carbohyd. Polym.* **2010**, *82*, 83.
34. Wang, W. B.; Zheng, Y. A.; Wang, A. Q. *Polym. Adv. Technol.* **2008**, *19*, 1852.
35. Chen, D. W.; Zhao, X. L.; Li, K. X.; Zhao, X. F.; Pang, D. H. *Chem. & Pharm. Bull.* **2008**, *56*, 963.
36. Zhang, J. P.; Wang, Q.; Wang, A. Q. *Acta Biomater.* **2009**, *6*, 445.
37. Jin, S. P.; Liu, M. Z.; Zhang, F.; Chen, S. L.; Niu, A. Z. *Polymer* **2006**, *47*, 1526.
38. Shu, X. Z.; Zhu, K. J.; Song, W. H. *Int. J. Pharm.* **2001**, *212*, 19.
39. Peppas, K. P.; Alexandropoulos, G. C.; Datsikas, C. K.; Lazarakis, F. I. *Iet Microw Antenna P* **2011**, *5*, 364.
40. Maswadeh, H. M.; Semreen, M. H. S.; Abdulhalim, A. A. *Acta Poloniae Pharmaceutica – Drug Research* **2006**, *63*, 63.
41. Desai, S. J.; Simonell, A.; Higuchi, W. I. *J. Pharm. Sci.* **1965**, *54*, 1459.
42. Siepmann, J.; Peppas, N. A. *Adv. Drug Deliv. Rev.* **2001**, *48*, 139.